Special Issue: Review

polymers advanced technologies

Received: 14 April 2010, Revised: 28 May 2010, Accepted: 30 May 2010, Published online in Wiley Online Library: 20 December 2010

(wileyonlinelibrary.com) DOI: 10.1002/pat.1781

Coaxial electrospinning and emulsion electrospinning of core–shell fibers

A.L. Yarin[a,b]*

The mini-review is devoted to coaxial electrospinning (co-electrospinning, emulsion electrospinning), a group of novel methods for making core–shell nanofibers and hollow nanotubes. The physical aspects of the process are described in brief, in particular, its modeling and possible drawbacks of the process resulting in formation of fibers without a long intact core. After that the main applications of co-electrospinning are considered. They include drug release, encapsulation of different biologically active compounds, cell scaffolds, formation of nanotubes, and nanofluidics. Copyright © 2010 John Wiley & Sons, Ltd.

Keywords: co-electrospinning, emulsion electrospinning, core–shell nanofibers, nanotubes, drug release, encapsulation, nanofluidics

Alexander Yarin received his MSc degree in Applied Physics from St. Petersburg State Polytechnic University in 1977. Then, he received PhD and DSc (habilitation) degrees in Physics and Mathematics from the Institute for Problems in Mechanics of the USSR Academy of Sciences in Moscow (in 1980 and 1989, respectively). In 1990–2005 he was Professor and Eduard Pestel Professor at the Technion-Israel Institute of Technology. From 2006 he is Professor at the University of Illinois at Chicago and a co-Director of the Micro- and Nanofluidics Laboratory. His research is related to transport phenomena in nanotechnology. He is the author of two books, seven book chapters and 190 peer-reviewed journal publications. Professor Yarin is a Co-editor of *Springer Handbook of Experimental Fluid Mechanics* (2007) and Associate Editor of the journal "Experiments in Fluids".

INTRODUCTION

Coaxial electrospinning or co-electrospinning of core–shell micro- and nanofibers was born 7 years ago as a branch of nanotechnology which bifurcated from a previously known electrospinning. Through electrospinning, co-electrospinning inherited roots in polymer science and electrohydrodynamics, while some additional genes from textile science and optical fiber technology were spliced in addition. Co-electrospinning also engulfed emulsion electrospinning. Co-electrospinning rapidly became widely popular and its applications proliferated into such fields as biotechnology, drug delivery and nanofluidics. It also triggered significant theoretical and experimental efforts directed at a better understanding and control of the process. As is usual with many modern nanotechnological processes, the situation reminds a babushka nested doll, with multiple interdisciplinary interactions exposed kaleidoscopically one by one and novel opportunities emerging down the road. The literature dealing with co-electrospinning and the kindred emulsion electrospinning already consists of hundreds of papers, several of them being reviews. Therefore, the current mini-review briefly outlines the basic features of the process and proceeds toward its deeper physical understanding, modifications, and recent applications.

FIRST STEPS OF CO-ELECTROSPINNING

Coaxial electrospinning (co-electrospinning) was introduced first in Reference [1]. It bifurcated from electrospinning, a widely popular process of making monolithic polymer nanofibers covered in several recent reviews.[2–4] Co-electrospinning introduced a novel class of nanofibers with core–shell structure. Similarly to electrospinning, co-electrospinning employs electric forces acting on polymer solutions in dc electric fields and resulting in significant stretching of polymer jets due to a direct pulling and growth of the electrically driven bending perturbations.[5,6] However, co-electrospinning was also motivated by such traditional fields as melt spinning of core–shell polymer fibers[7] and formation of polarization-maintaining core–shell optical glass fibers.[8] It is worth mentioning that electrically driven core–shell jets also emerge in electrospraying,[9] albeit the hydrodynamic issues and the products of the latter process are completely different. In the case of electrospraying, the jets should be rapidly atomized into tiny core–shell droplets, with no viscoelasticity or jet bending involved, whereas in the case of co-electospinning, polymer jet should stay intact to make

* *Correspondence to: A. Yarin, Department of Mechanical and Industrial Engineering, University of Illinois at Chicago, 842 W Taylor St., Chicago IL 60607-7022, USA.*
E-mail: ayarin@uic.edu

a *A. Yarin*
Department of Mechanical and Industrial Engineering, University of Illinois at Chicago, 842 W Taylor St., Chicago IL 60607-7022, USA

b *A. Yarin*
Center for Smart Interfaces, Technische Universität Darmstadt, Petersenstr. 32, 64287 Darmstadt, Germany

polymers advanced technologies

nanofibers, and viscoelasticity and jet bending are the dominant phenomena.

In co-electrospinning, a plastic syringe with two compartments containing different polymer solutions or a polymer solution (shell) and a non-polymeric Newtonian liquid or even a powder (core) is used to initiate a core–shell jet (Fig. 1a). At the exit of the core–shell needle attached to the syringe appears a core–shell droplet, which acquires a shape similar to the Taylor cone due to the pulling action of the electric Maxwell stresses acting on liquid.[10] Liquid in the cone, being subjected to sufficiently strong (supercritical) electric field, issues a compound jet, which undergoes the electrically driven bending instability characteristic of the ordinary electrospinning process.[1–3] Strong jet stretching resulting from the bending instability is accompanied by enormous jet thinning and fast solvent evaporation. As a result, the core–shell jet solidifies and core–shell fibers are depositing on a counter-electrode. Some polymer pairs can result in core–shell nanofibers (Fig. 1b—polysulfone/(polyoxyethylene)), some others in microfibers (Fig. 1c—poly(methyl methacrylate)/polyacrylonitrile).

Co-electrospinning rapidly gained popularity and was implemented by a number of groups.[13–18] A comprehensive review of the first stage of evolution of co-electrospinning is available.[12]

NEW IDEAS: CO-ELECTROSPINNING FROM A SINGLE NOZZLE

Conventional co-electrospinning requires a core–shell nozzle attached to a double-compartment syringe of Fig. 1(a) or supply of two polymer solutions by means of two separate syringe pumps and pipelines leading to a core–shell nozzle. Therefore, co-electrospinning setups are more complicated than the ordinary electrospinning ones which involve a single nozzle and pump.[2,3] However, recently it was demonstrated that co-electrospinning of core–shell polymer nanofibers is possible from an ordinary single-nozzle electrospinning setup if an emulsion of two polymer solutions is used as a working liquid.[19] Solutions of PMMA in DMF and PAN in DMF were blended and left for one day. During that time the blend decomposed into PMMA/DMF droplets of about 100 μm in diameter dispersed in PAN/DMF matrix. The resulting emulsion was electrospun using an ordinary electrospinning setup (Fig. 2a, left). In this case core–shell Taylor cone at the nozzle exit is only transient: it appears periodically when a PMMA/DMF droplet is entrained into the tip of a single-liquid Taylor cone created by PAN/DMF matrix (Fig. 2a, right). A core–shell jet is issued from a transient compound core–shell Taylor cone only during the time of its existence before the PMMA/DMF droplet trapped in its tip expires. Therefore, in principle, the as-spun fibers should not possess an intact PMMA core. However, as found by inspecting the as-spun fibers (cf. Fig. 2b), the number of core disruptions is very small. The reason for that is in a very strong stretching of material elements in the co-electrospun jet. For example, the length of a fiber section of diameter $d \sim 1$ μm co-electrospun from one trapped PMMA/DMF droplet of diameter $D \sim 100$ μm should be about $D^3/d^2 \sim 1$ m.

For the employed flow rates, it is estimated that PMMA/DMF droplet is consumed within a few milliseconds. This is significantly longer than the charge relaxation time of such polymer solutions. Therefore, all the electric charges have enough time to escape to the free (outer) surface of the compound Taylor cone. As a result, stretching of the tip of the PMMA/DMF droplet currently trapped in the Taylor cone (Fig. 2a, right) is due to strong suction (a negative pressure, traction) there, which is related to viscous forces alone.

The as-spun fibers obtained in Reference [19] had the outer diameters in the range 0.5–5 μm and possessed core–shell structure (Fig. 2b), similar to that attained via core–shell nozzles. Co-electrospinning of core–shell nano- and microfibers from a single nozzle was also implemented in several following works.[20–23] Sometimes the process is termed as the emulsion electrospinning[24,25] and viewed as an agglomeration of droplets in the core of the emulsion jet.[25] This scenario can hardly be realized, and the realistic physical mechanism is depicted in Fig. 2(a). Moreover, it is emphasized that the emulsion electrospinning in many cases does not result in core–shell polymer fibers but rather in fibers with dispersed phase embedded as separate blobs. These cases are not termed as co-electrospinning according to our definition. Only those cases, which result in core–shell fibers with a very long continuous core, as was recognized in Reference [19], represent themselves the part of the emulsion electrospinning engulfed by co-electrospinning and thus covered in the present mini-review.

THEORETICAL WORKS ON CO-ELECTROSPINNING

Several theoretical works dealt with different aspects of co-electrospinning with the goal of better understanding its

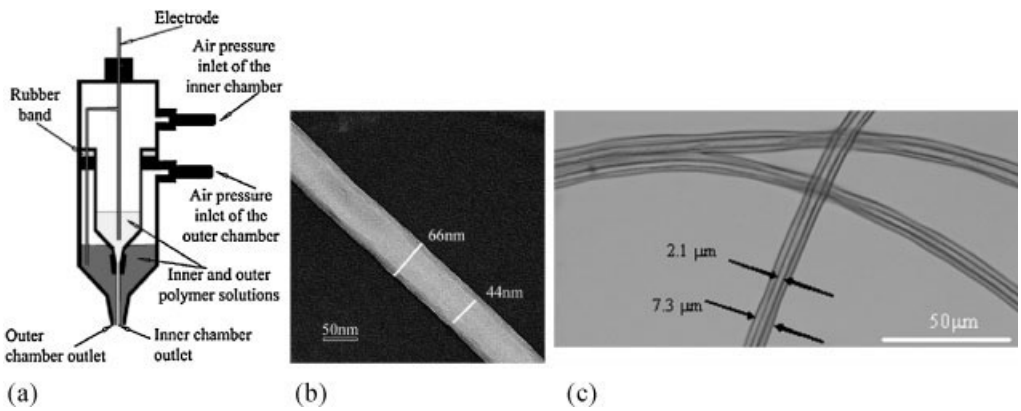

Figure 1. Coaxial electrospinning. (a) A double-compartment plastic syringe for co-electrospinning features separate supplies of core and shell materials. (b) TEM micrograph of a core–shell nanofiber. The core and shell solutions are PSU and PEO, respectively. (c) Optical image of core–shell microfibers. The core and shell solutions are PMMA and PAN, respectively. With permission from References [1,11,12] (Courtesy of John Wiley&Sons).

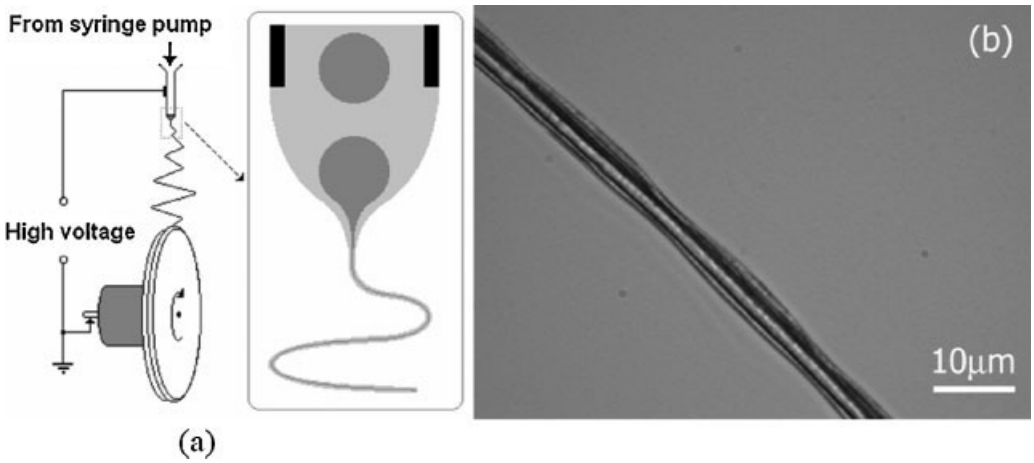

Figure 2. (a) Emulsion co-electrospinning of PMMA/PAN blend in DMF using a single nozzle. The inset (right) shows magnified detail of the needle orifice, which is shown in black on top. The PMMA/DMF droplets are shown in dark gray, whereas the PAN/DMF matrix is lighter. The core–shell fibers are collected on the edge of the rotating wheel serving as a grounded electrode. (b) Optical images of as-spun core–shell microfibers collected on a glass slide located between the electrodes. The fiber has the largest diameter produced by this method, since fiber stretching at the location of the collecting glass slide had not terminated yet. With permission from Reference [19] (Courtesy of the American Chemical Society).

underlying physics and enhancing its efficiency. Using core–shell nozzles does not necessarily imply formation of core–shell jets. The core material may be not entrained into the shell jet, which results in monolithic instead of core–shell jets.[10] The detailed numerical simulations[10] of flows developing in a core–shell droplet at the exit of a core–shell nozzle under the action of the pulling electric Maxwell stresses showed that the electric charges very rapidly escape to the outer surface of the forming jet. As a result, core entrainment is possible only due to viscous tractions. The core entrainment was predicted to be facilitated by a core nozzle protruding from a coaxial shell nozzle,[10] which was demonstrated experimentally.[11]

Viscous tractions are also responsible for formation of core–shell jets in the case of the emulsion electrospinning from PMMA-PAN blends (Fig. 3).[19] Indeed, in the proximity of the Taylor cone (Fig. 2a, right), the angular spherical coordinate reckoned from the cone tip $\theta << 1$, whereas the pressure distribution over the PMMA droplet surface is given by[19]

$$p = -\frac{3\mu Q}{2\pi\varepsilon^3(1-\lambda)^3}\ln\theta \qquad (1)$$

where $\lambda = e/\varepsilon < 1$ (with e being the displacement between the centers of the PAN and PMMA droplets at the tip, and ε the difference between the radii of the PAN, outer, and PMMA, inner, droplets); Q is the volumetric flow rate corresponding to the syringe pump considered to be negative and μ the zero-shear viscosity of the PAN solution in this flow. According to eqn (1), the pressure $p < 0$, which means that the surface of the PMMA droplet is pulled downward (Fig. 2a, right). It is emphasized that the shear stress $\tau_{r\theta}$ (r is the radial spherical coordinate) at the surface of the PAN droplet entrapped at the Taylor cone tip is much lower than the pressure p, since $\tau_{r\theta}/p = O(\varepsilon/R) << 1$, where R is the droplet radius ($R >> \varepsilon$). This means that the viscous shear stress can be safely neglected and the trapped drop will be affected only by the pulling effect of the negative pressure (suction, traction). According to eqn (1), pulling at the surface of the inner PMMA droplet becomes very strong in the vicinity of the Taylor cone where $\theta << 1$. An average pressure over the section $0 < \theta < \theta^* << 1$ is $P = -3\mu Q/[2\pi\varepsilon^3(1-\lambda)^3](\ln\theta^* - 1)$.

The viscoelastic response of the PMMA solution in the trapped droplet should be predominantly elastic and governed by the momentum balance $2G(L/l)^2 = -P$, where G is the elasticity modulus of the PMMA/DMF solution and L/l is the stretching ratio at the drop tip. The latter yields $L/l \sim [\mu(-Q)/\varepsilon^3 G]^{1/2}$. Therefore, PMMA solutions with lower G, and PAN solutions with higher μ, as well as flows with higher Q, would result in easier stretching and thinning of the PMMA core and, in turn, facilitate formation of core–shell fibers in the emulsion electrospinning (G and μ can be varied by manipulating molecular weight and concentration). Introducing the viscoelastic relaxation time as $\vartheta \sim \mu/G$, the stretching ratio can be written as $L/l \sim [(-Q)\,\vartheta/\varepsilon^3]^{1/2}$. Taking the estimate: — $Q \sim 1$ ml/hr, $\vartheta \sim 0.1$ sec, and $\varepsilon \sim 0.5 \times 10^{-2}$ cm, one can deduce $L/l \sim 10$, which indicates a high stretching ratio, suggesting that the PMMA/DMF droplet can be pulled into the

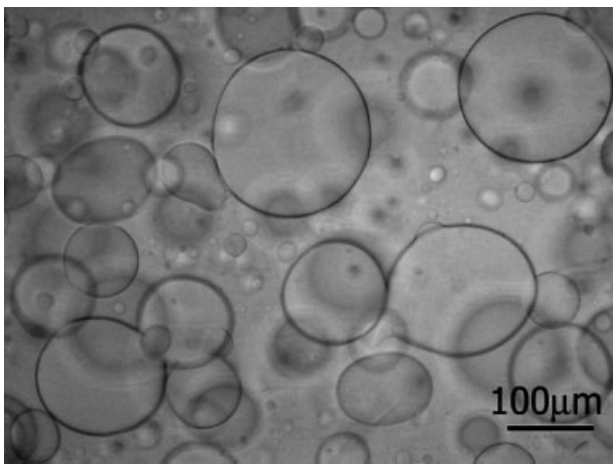

Figure 3. PMMA/PAN emulsion about 1 day after mixing equal amounts of each polymer in DMF to create a homogeneous blend containing 6 wt% PMMA and 6 wt%. PAN. The PMMA/DMF droplets are dispersed in the surrounding PAN/DMF matrix. With permission from Reference [19] (Courtesy of the American Chemical Society).

PAN/DMF jet, thus leading to formation of a core–shell jet and the subsequent formation of core–shell fibers.

After being formed, core–shell jets are prone to a number of instabilities. First of all, the whole process of co-electrospinning and drastic thinning of core–shell jets is rooted in the electrically driven bending instability associated with bending perturbations familiar from the theory of an ordinary electrospinning process.[2,5,26] In the context of co-electrospinning a number of works was devoted to the dynamics of growth of small perturbations, and in particular, small bending perturbations.[27–31] However, there is still no adequate fully nonlinear theory of bending of electrically driven, viscoelastic core–shell jets similar to that for the monolithic ones.[2,5,26] If viscoelastic properties (zero-shear viscosity and relaxation time) and density of the core and shell polymer solutions are almost identical, the existing nonlinear theory for monolithic jets can be directly applied in the case of co-electrospinning or the emulsion electrospinning of core–shell fibers. However, if a disparity in the properties is significant, a more general description is still to be developed.

Core–shell jets can also be prone to capillary instabilities of two types. The first one is the regular capillary instability where the viscoelastic forces are insufficient (typically, if polymer solutions are rather dilute) to prevent it, and the whole jet breaks up into droplets as any monolithic jet would. This type of capillary instability is driven by surface tension of the shell liquid, albeit can also be affected by the electric forces to some extent. In the less severe cases this type of capillary instability results in a visible waviness of the outer surface of the shell similar to the one seen in Fig. 2(b). The second type of capillary instability is specific for core–shell jets. In this case, the interfacial tension plays the leading role and the core breaks up into separate droplets inside of an intact shell. In this case co-electrospinning begins from a core–shell jet but results in a compound jet with no intact core. The direct numerical simulations of straight core–shell jets[32] shed some light on the core breakup pattern. It is emphasized that in the emulsion electrospinning from a single nozzle there might be cases where core–shell jet does not exist at all and droplets of the dispersed phase in emulsion are just sucked into the matrix jet resulting in fibers with beads in the core. This outcome might be even desirable.[24,33]

Core–shell jets in co-elecrospinning can demonstrate some additional forms of instabilities leading to imperfections of the as-spun fibers. The core and shell polymer solutions can have a relative velocity, which results from different supply rates determined independently for two syringe pumps. As a result, there might be a distributed longitudinal compression force imposed on the core. Then, the core can buckle[11] (Fig. 4a). A buckled core can even protrude from the surrounding shell resulting in arches revealed in experiments (Fig. 4b).[11] A theory of buckling which allows for prediction of the wavelength of the buckled core is available.[11] It predicts the characteristic buckling "steps" (cf. Fig. 4a) as

$$\frac{\Delta L_{i,i+1}}{a} = K \times \left(\left| U_{*,i+1} \right|^{3/4} - \left| U_{*,i} \right|^{3/4} \right) \tag{2}$$

where $U_{*,i} = -4.233, -7.86, -11.49,\ldots$ ($i = 1, 2, 3,\ldots$) are the roots of the equation

$$\exp\left(\frac{3}{2}U_*\right) = \sqrt{3}\sin\left(\frac{\sqrt{3}}{2}U_*\right) + \cos\left(\frac{\sqrt{3}}{2}U_*\right) \tag{3}$$

where a is the core cross-sectional radius, and the dimensionless factor K is dependent on the ratio A/a, where A is the shell cross-sectional radius.

Due to rapid evaporation of solvent from the core in co-electrospinning (and even in the ordinary electrospinning of monolithic fibers), a practically hollow core can emerge in the

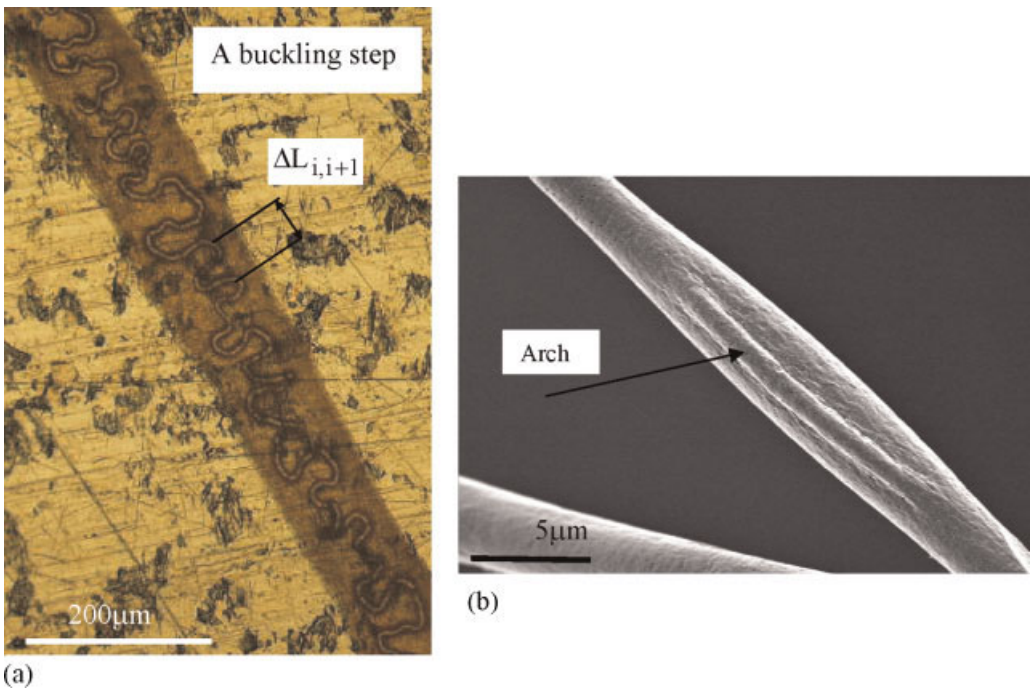

Figure 4. (a) Optical images of collected core–shell microfibers with buckling of the core jet inside the shell (the fibers are resting on an aluminum substrate). (b) Optical image of core–shell fibers, with the outer fiber (shell) diameter of around 7 μm and the core diameter of about 2 μm. With permission from Reference [11] (Courtesy of John Wiley&Sons). This figure is available in color online at www.interscience.wiley.com/journal/pat

jet in flight. Such hollow jets are subjected to the lateral compressive pressure differential and are prone to collapse, which results in ribbons rather than in cylindrical fibers.[34,35] The theoretical aspects of jet lateral collapse are similar to those of laterally loaded cylindrical shells and were first considered in Reference [12]. A further development of the theory accounting for the rate of the evaporation process is available in Reference [36].

APPLICATIONS OF CO-ELECTROSPINNING FOR ENCAPSULATION OF BIOLOGICALLY ACTIVE COMPOUNDS, CELL SCAFFOLDS, AND DRUG RELEASE

After its introduction, co-electrospinning rapidly became popular and is used by many research groups for different purposes. In particular, co-electrospinning allows encapsulation in the nanofiber core or wrapping as a shell of non-spinnable polymers, or non-polymeric materials like powders, nanoparticle suspensions, catalysts, proteins, as well as Type I collagen, gelatin, liquid crystals and monomers, which can be further chemically transformed or polymerized.[1,12,17,18,35,37–49] This can be considered as a modified version of the so-called host–guest approach used to electrospin blends of spinnable polymers with poorly spinnanble or non-spinnable conducting polymers.[2,50]

One of possible motivations for applying co-electrospinning is to modify wettability properties of nanofiber surface,[51,52] for example, using Teflon solution as a shell-forming material,[52] or to make nanofibers "friendly" as cell scaffolds.[39,44] Numerous works dealt with applying co-electrospinning for encapsulation of drugs or biologically active objects in the fiber core.[12,33,35,51,53–64] This approach is basically motivated by two ideas: to control the release rate by a shell used as a buffer (in particular, to suppress the initial burst release), or to protect biologically active agents in the core from harsh solvents of the spinnable polymer solution in the shell. However, it was shown[60] that the release rate from nanofibers is controlled not by solid-state diffusion, as it was widely assumed before, but rather by desorption of the admixture molecules from the surfaces directly exposed to the surrounding water. As a result, the admixture contained in the nanofiber bulk, in particular, in the core surrounded by a perfectly intact shell, practically cannot be released. To overbear this obstacle, porogens (materials which rapidly dissolve in water, leaving open pores: typically, (poly)-ethylene glycol, PEG) are added in the shell,[53,57,58] or biodegradable shells are used. This facilitates and regulates drug release from the core. Otherwise, release from the core is possible only due to the presence of different shell imperfections (cracks, throughout pores, etc.).[59]

On the other hand, protection of biologically active objects in the core of co-electrospun nanofibers does work, and a significant proportion of them stays viable in the as-spun fibers.[12,35,55,59,63] They are protected in the core not only from the harsh solvents in the shell solution but also from the effect of the electric charges, since the latter rapidly escape to the outer surface of the shell at the very beginning of core–shell jet formation.[10] Still, mechanical stresses at the interface between the core and shell solutions at the initiation of co-electrospinning were predicted to be of the order of 500 Pa, which approaches the lower level of mechanical stresses lethal to many biologically active agents (10^3–10^5 Pa).[12]

FORMATION OF NANOTUBES AND NANOFLUIDICS

Almost from the very beginning, one of the main aims of co-electrospinning was in formation of nanotubes. Precursors appropriate for a further sol-gel transformation of nanofibers at the post-processing calcination stage were blended in shell solutions, which allowed their conversion into ceramic tubes, while core was removed chemically.[13,14,18,65–69] These ceramic tubes, however, were never used in nanofluidic devices, as to our knowledge. On the other hand, co-electrospinning of core–shell nanofibers with PMMA solution in the core and PAN solution in the shell opened way to production of robust long carbon nanotubes appropriate for nanofluidic applications.[11,19] At the post-processing heat treatment stage PMMA in the core was completely eliminated, whereas PAN in the shell carbonized resulting in turbostratic amorphous carbon nanotubes, which are stiff enough to sustain pressures of the order of 10 bar in the bore. Formation of nanotubes en masse by such a relatively cheap method as co-electrospinning promises some benefits compared to the traditional methods of microfabrication.

The first efforts to demonstrate flows inside hollow polymer microtubes formed via co-electrospinning were undertaken in Reference [35], where the tubes were filled with water, and wettability- and evaporation-driven motion of meniscus in the bore was observed. Then, pressure driven-flows inside co-electrospun and carbonized micro- and nanotubes were demonstrated.[70,71] In the latter two works, at the co-electrospinning stage, core–shell fibers were collected as parallel bundles of about 40 000 fibers using the method of the electrostatic lens (a sharp vertical grounded wheel).[2,72,73] After carbonization, these bundles were converted into bundles of parallel carbon nanotubes (Fig. 5) sufficiently long to be installed manually into a pressure-driven nanofluidic device (Fig. 6). They were able to sustain pressure-driven flows of air and liquids, which was visualized by release into Petri dish filled with an immiscible liquid (Fig. 7). In the cases shown in Fig. 7, micro-bubbles and micro-droplets released from individual tubes merged and formed macroscopic bubbles or drops used to measure the overall release rate. On the other hand, the addition of surfactants allows one to keep micro-droplets mostly apart and prevent their agglomeration into big clusters (merger drops). Then, similar bundles can be used for production of therapeutically valuable nanoparticles at rates of the order of 10^7 particles per second.[74]

Such issues as clogging of co-electrospun carbon nanotubes, which are relevant for long-term drug delivery devices, were addressed in Reference [71].

CONCLUSION AND OUTLOOK

The physical mechanisms of co-electrospinning and emulsion electrospinning of core–shell fibers are pretty well understood. However, a fully theoretical prediction of the outcome and robustness of a particular process is still impossible due to the presence of many governing parameters which are not fully known or controlled (e.g. rheological behavior and the electric

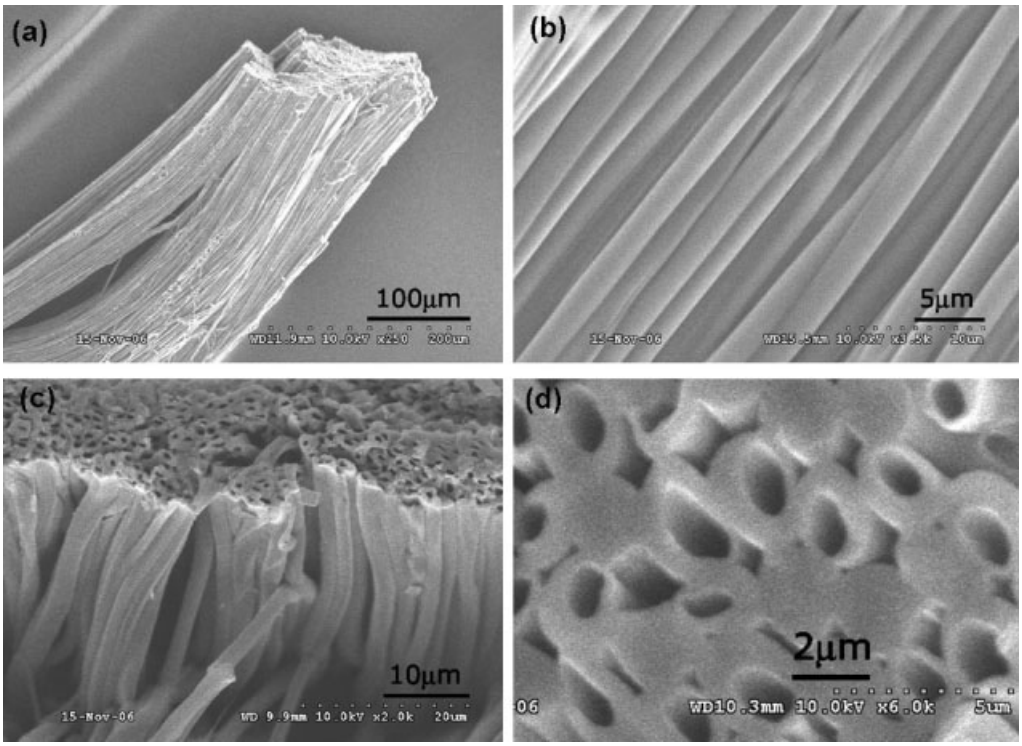

Figure 5. SEM images of a bundle of carbon tubes made via co-electrospinning. Longitudinal views at low (a) and high (b) magnification. Low (c) and high (d) magnification cross-sectional views of the end of the bundle. The large gap shown in the top middle of (c) is a result of handling. Some non-hollow fibers seen in (d) could have been created by intermittent co-electrospinning, or could indicate tube ends crimped during cutting of the bundle. With permission from Reference [70] (Courtesy of the Royal Society of Chemistry).

properties of polymer solutions are rarely characterized prior to the experiments). This requires a number of trials before a particular process begins yielding satisfactory results, which poses a potential challenge to wide-scale industrial implementations (similarly to the ordinary electrospinning process). Development of co-electrospinning machines for industrial applications should probably be more challenging than in the case of an ordinary electrospinning.

Extrapolating the current tendencies, one can expect that the innovative technological ideas springing from co-electrospinning will most probably encompass in future such applications as cell scaffolds and release of growth factors for stem cell differentiation, catalytic and polymerization nanoreactors, drug releasing implants and nanofluidic devices for long-term drug delivery.

Co-electrospinning allows a straightforward way of manipulating wettability properties of fibers, e.g. making them fully wettable, or on the opposite, non-wettable. This issue might be discussed in relation to development of novel water and/or oil repelling filters. However, static wettability of electrospun non-woven filters is determined mostly by the presence of air

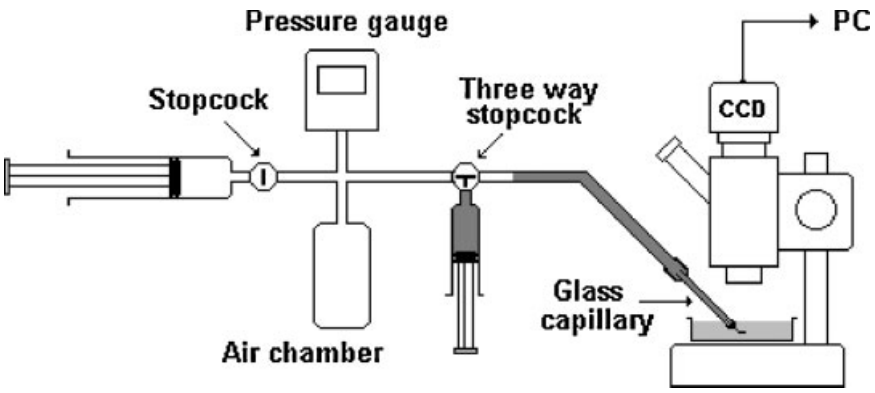

Figure 6. Sketch of the experimental nanofluidic setup. The carbon nanotube bundle is secured by inert epoxy cement at the exit of a glass capillary and submerged in a Petri dish containing water or oil. The fluid supply system consists of two standard plastic syringes of volumes 10 and 1 ml, a digital pressure gauge, a 7-ml plastic air chamber and two stopcocks connected by thin silicon tubing. The air chamber is used to maintain pressure at a nearly constant level during the release experiments. After pressurizing the air chamber by means of the 10-ml syringe (on the left in the figure), the one-way stopcock is closed. The second syringe (vertical in the figure), which is connected directly to the three-way stopcock, is used to fill (with oil or water) the silicon pipe leading to the glass capillary and the nanotubes. With permission from Reference [70] (Courtesy of the Royal Society of Chemistry).

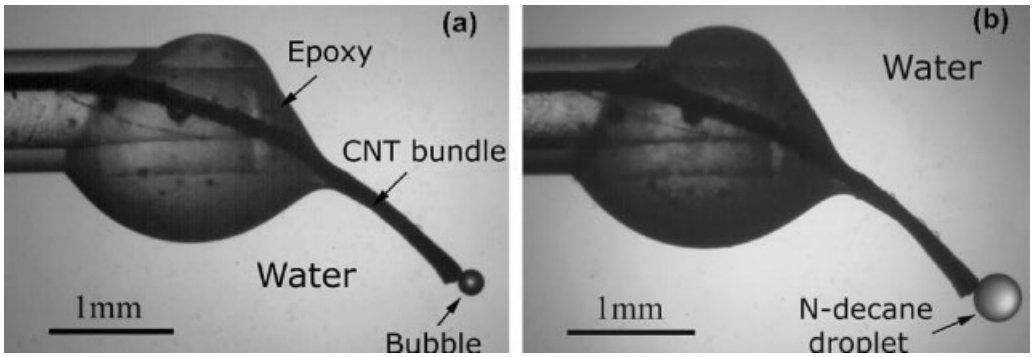

Figure 7. (a) Growing merger air bubble at the tip of the carbon tube bundle immersed in a shallow water pool in Petri dish (Fig. 6). (b) Growing merger *n*-decane droplet in a water pool. With permission from Reference [70] (Courtesy of the Royal Society of Chemistry).

in the pores, which constitute porosity of about 90–95%. The presence of air results in the Cassie–Baxter-like situation and a superhydrophobic-like appearance of droplets softly deposited on such filters.[75] On the other hand, drop impacts almost inevitably result in liquid penetration into pores irrespective of fiber wettability properties,[75] which corresponds to an enforced Wenzel-like situation. The latter shows that creation of water and/or oil repelling filters by means of the fiber wettability manipulation is far from being guaranteed and deserves further research efforts. In addition, co-electrospinning of filter media with the fiber shells consisting of water-insoluble, thermo-responsive hydrogels[76] could probably open way for development of self-cleaning filters capable of shaking loose fouling layers.

New application areas would be covered if a robust co-electrospinning of hollow nanotubes with the outer diameters below 100 nm could be achieved, and spectrum of wall materials widen beyond ceramics and carbon (e.g. making robust and relatively smooth metal nanotubes). Co-electrospinning has good chances to become a key part of the innovative non-woven technology for producing fibers with the islands-in-the-sea cross-sectional structure.[77] It can be also used for production of multichannel nanotubes. Nanotubes and nanotube non-woven webs made via co-electrospinning deserve attention of specialists dealing with thermal management of microelectronic devices (cf. Reference [78]). Being basically a simple and cheap process, co-electrospinning can conquer a permanent niche under the umbrella of nanotechnology.

Acknowledgements

The author is grateful for partial support of his work by National Science Foundation through Grant NIRT CBET-0609062.

REFERENCES

[1] Z. Sun, E. Zussman, A. L. Yarin, J. H. Wendorff, A. Greiner, *Adv. Mater.* **2003**, *15*, 1929–1932.
[2] D. H. Reneker, A. L. Yarin, E. Zussman, H. Xu, *Adv. Appl. Mech.* **2007**, *41*, 43–195.
[3] D. H. Reneker, A. L. Yarin, *Polymer* **2008**, *49*, 2387–2425.
[4] S. Agarwal, A. Greiner, J. H. Wendorff, *Adv. Funct. Mater.* **2009**, *19*, 2863–2879.
[5] D. H. Reneker, A. L. Yarin, H. Fong, S. Koombhongse, *J. Appl. Phys.* **2000**, *87*, 4531–4547.
[6] T. Han, A. L. Yarin, D. H. Reneker, *Polymer* **2008**, *49*, 1651–1658.
[7] A. Ziabicki, *Fundamentals of Fibre Formation*, Wiley, London, **1976**.
[8] A. L. Yarin, *J. Fluid Mech.* **1995**, *286*, 173–200.
[9] I. G. Loscertales, A. Barrero, I. Guerrero, R. Cortijo, M. Marquez, A. M. Ganan-Calvo, *Science* **2002**, *295*, 1695–1698.
[10] S. N. Reznik, A. L. Yarin, E. Zussman, L. Bercovici, *Phys. Fluids* **2006**, *18*, 062101.
[11] E. Zussman, A. L. Yarin, A. V. Bazilevsky, R. Avrahami, M. Feldman, *Adv. Mater.* **2006**, *18*, 348–353.
[12] A. L. Yarin, E. Zussman, J. H. Wendorff, A. Greiner, *J. Mater. Chem.* **2007**, *17*, 2585–2599.
[13] D. Li., Y. Xia, *Nano Lett.* **2004**, *4*, 933–938.
[14] D. Li, Y. Xia, *Adv. Mater.* **2004**, *16*, 1151–1170.
[15] I. G. Loscertales, A. Barrero, M. Marquez, R. Spretz, R. Velarde-Ortiz, G. Larsen, *J. Am. Chem. Soc.* **2004**, *126*, 5376–5377.
[16] J. H. Yu, S. V. Fridrikh, G. C. Rutledge, *Adv. Mater.* **2004**, *16*, 1562–1566.
[17] Y. Zhang, Z. M. Huang, X. Xu, C. T. Lim, S. Ramakrishna, *Chem. Mater.* **2004**, *16*, 3406–3409.
[18] D. Li, J. T. McCann, Y. Xia, *Small* **2005**, *1*, 83–86.
[19] A. V. Bazilevsky, A. L. Yarin, C. M. Megaridis, *Langmuir* **2007**, *23*, 2311–2314.
[20] X. H. Li, C. L. Shao, Y. C. Liu, *Langmuir* **2007**, *23*, 10920–10923.
[21] C. Kim, Y. I. Jeong, B. T. N. Ngoc, K. S. Yang, M. Kojima, Y. A. Kim, M. Endo, J. W. Lee, *Small* **2007**, *3*, 91–95.
[22] C. K. Hong, K. S. Yang, S. H. Oh, J. H. Ahn, B. H. Cho, C. Nah, *Polym. Int.* **2008**, *57*, 1357–1362.
[23] J. F. Zhang, D. Z. Yang, F. Xu, Z. P. Zhang, R. X. Yin, J. Nie, *Macromolecules* **2009**, *42*, 5278–5284.
[24] M. Angeles, H. L. Cheng, S. S. Velankar, *Polym. Adv. Technol.* **2008**, *19*, 728–733.
[25] X. L. Xu, X. L. Zhuang, X. S. Chen, X. Wang, L. Yang, X. Jing, *Macromol. Rapid Commun.* **2006**, *27*, 1637–1642.
[26] A. L. Yarin, S. Koombhongse, D. H. Reneker, *J. Appl. Phys.* **2001**, *89*, 3018–3026.
[27] F. Li, X. Y. Yin, X. Z. Yin, *Phys. Fluids* **2005**, *17*, 077104.
[28] F. Li, X. Y. Yin, X. Z. Yin, *Phys. Fluids* **2006**, *18*, 037101.
[29] F. Li, X. Y. Yin, X. Z. Yin, *Phys. Rev. E* **2006**, *74*, 036304.
[30] F. Li, X. Y. Yin, X. Z. Yin, *Phys. Rev. E* **2008**, *78*, 036302.
[31] F. Li, X. Y. Yin, X. Z. Yin, *J. Fluid Mech.* **2009**, *632*, 199–225.
[32] Y. Y. Hu, Z. M. Huang, *J. Appl. Phys.* **2007**, *101*, 084307.
[33] H. X. Qu, P. Hu, J. Xu, A. Wang, *Biomacromolecules* **2006**, *8*, 2327–2330.
[34] S. Koombhongse, W. Liu, D. H. Reneker, *J. Polym. Sci. Polym. Phys. Ed.* **2001**, *39*, 2598–2606.
[35] Y. Dror, W. Salalha, R. Avrahami, E. Zussman, A. L. Yarin, R. Dersch, A. Greiner, J. H. Wendorff, *Small* **2007**, *3*, 1064–1073.
[36] A. Arinstein, R. Avrahami, E. Zussman, *J. Phys. D Appl. Phys.* **2009**, *42*, 015507.
[37] J. T. McCann, D. Li, Y. N. Xia, *J. Mater. Chem.* **2005**, *15*, 735–738.
[38] T. Song, Y. Z. Zhang, T. J. Zhou, C. T. Lim, S. Ramakrishna, B. Liu, *Chem. Phys. Lett.* **2005**, *415*, 317–322.
[39] Y. Z. Zhang, J. Venugopal, Z. M. Huang, C. T. Lim, S. Ramakrishna, *Biomacromolecules* **2005**, *6*, 2583–2589.
[40] B. Sun, B. Duan, X. Y. Yuan, *J. Appl. Polym. Sci.* **2006**, *102*, 39–45.
[41] C. Burger, B. S. Hsiao, B. Chu, *Ann. Rev. Mater. Res.* **2006**, *36*, 333–368.
[42] P. C. Zhao, H. L. Jiang, H. Pan, K. Zhu, W. Chen, *J. Biomed. Res. A* **2007**, *83*, 372–382.

[43] Q. Zhao, Y. Xin, Z. H. Huang, S. Liu, C. Yang, Y. Li, *Polymer* **2007**, *48*, 4311–4315.
[44] P. Zhao, H. Jiang, H. Pan, K. Zhu, W. Chen, *J. Biomed. Mater. Res. A* **2007**, *83*, 372–382.
[45] F. Yi, D. A. LaVan, *Mol. Biosci.* **2008**, *8*, 803–806.
[46] Y. Xin, Z. H. Huang, W. W. Li, Z. Jiang, Y. Tong, C. Wang, *Eur. Polym. J.* **2008**, *44*, 1040–1045.
[47] J. P. F. Lagerwall, J. T. McCann, E. Formo, G. Scalia, Y. Xia, *Chem. Commun.* **2008**, *42*, 5420–5422.
[48] V. Thavasi, G. Singh, S. Ramakrishna, *Energy Environ. Sci.* **2008**, *1*, 205–221.
[49] C. R. Reddy, A. Arinstein, R. Avrahami, E. Zussman, *J. Mater. Chem.* **2009**, *19*, 7198–7201.
[50] M. Wei, J. Lee, B. W. Kang, J. Mead, *Macromol. Rapid Commun.* **2005**, *26*, 1127–1132.
[51] J. E. Diaz, A. Barrero, M. Marquez, I. G. Loscertales, *Adv. Funct. Mat.* **2006**, *16*, 2110–2116.
[52] D. Hand, A. J. Steckl, *Langmuir* **2009**, *25*, 9454–9462.
[53] H. L. Jiang, Y. Q. Yu, Y. Li, P. Zhao, K. Zhu, W. Chen, *J. Control. Release* **2005**, *108*, 237–243.
[54] Z. M. Huang, C. L. He, A. Yang, Y. Zhang, X. J. Han, J. Yin, Q. Wu, *J. Biomed. Mater. Res. A* **2005**, *77*, 169–179.
[55] A. Greiner, J. H. Wendorff, A. L. Yarin, E. Zussman, *Appl. Microbiol. Biotechnol.* **2006**, *71*, 387–393.
[56] W. Salalha, J. Kuhn, Y. Dror, E. Zussman, *Nanotechnology* **2006**, *17*, 4675–4681.
[57] H. L. Jiang, Y. Q. Hu, P. C. Zhao, Y. Li, K. Zhu, *J. Biomed. Mater. Res. B Appl. Biomater.* **2006**, *79B*, 50–57.
[58] Y. Z. Zhang, X. Wang, Y. Feng, J. Li, C. T. Lim, S. Ramakrishna, *Biomacromolecules* **2006**, *7*, 1049–1057.
[59] Y. Dror, J. Kuhn, R. Avrahami, E. Zussman, *Macromolecules* **2008**, *41*, 4187–4192.
[60] R. Srikar, A. L. Yarin, C. M. Megaridis, A. V. Bazilevsky, E. Kelley, *Langmuir* **2008**, *24*, 965–974.
[61] C. L. He, Z. M. Huang, X. J. Han, *J. Biomed. Mater. Res. A* **2008**, *89*, 80–95.
[62] A. Saraf, G. Lozier, A. Haesslein, F. K. Kasper, R. M. Raphael, L. C. Baggett, A. G. Mikos, *Tissue Eng. C* **2009**, *15*, 333–344.
[63] A. Lopez-Rubio, E. Sanchez, Y. Sanz, J. M. Lagaron, *Biomacromolecules* **2009**, *10*, 2823–2829.
[64] E. Jo, S. W. Lee, K. T. Kim, Y. S. Won, H. S. Kim, E. C. Cho, U. Jeong, *Adv. Mater.* **2009**, *21*, 968–972.
[65] V. Kalra, S. Mendez, J. H. Lee, N. Nguyen, M. Marquez, Y. L. Joo, *Adv. Mater.* **2006**, *18*, 3299–3303.
[66] Y. X. Gu, D. R. Chen, X. L. Jiao, F. Liu, *J. Mater. Chem.* **2007**, *17*, 1769–1776.
[67] S. H. Zhan, D. R. Chen, X. L. Jiao, S. Liu, *J. Colloid Interface Sci.* **2007**, *308*, 265–270.
[68] Y. X. Gu, F. F. Jian, *J. Phys. Chem. C* **2008**, *112*, 20176–20180.
[69] J. C. Di, H. Y. Chen, X. F. Wang, Y. Zhao, L. Jiang, J. Yu, R. Xu, *Chem. Mater.* **2008**, *20*, 3543–3545.
[70] A. V. Bazilevsky, A. L. Yarin, C. M. Megaridis, *Lab Chip* **2008**, *8*, 152–160.
[71] R. Srikar, A. L. Yarin, C. M. Megaridis, *Nanotechnology* **2009**, *20*, 275706.
[72] A. Theron, E. Zussman, A. L. Yarin, *Nanotechnology* **2001**, *12*, 384–390.
[73] E. Zussman, A. Theron, A. L. Yarin, *Appl. Phys. Lett.* **2003**, *82*, 973–975.
[74] S. Sinha-Ray, A. L. Yarin, *J. Appl. Phys.* **2010**, *107*, 0294903.
[75] A. Lembach, H. B. Tan, I. V. Roisman, T. Gambaryan-Roisman, Y. Zhang, C. Tropea, A. L. Yarin, *Langmuir* **2010**, *26*, 9516–9523.
[76] Y. Zhang, A. L. Yarin, *J. Mater. Chem.* **2009**, *19*, 4732–4739.
[77] A. Durany, N. Anantharamaiah, B. Pourdeyhimi, *J. Mater. Sci.* **2009**, *44*, 5926–5934.
[78] R. Srikar, T. Gambaryan-Roisman, C. Steffes, P. Stephan, C. Tropea, A. L. Yarin, *Int. J. Heat Mass Transf.* **2009**, *52*, 5814–5826.

